SEISMIC PERFORMANCE COMPARISON OF BASE-ISOLATED HOSPITAL BUILDING WITH VARIOUS ISOLATOR MODELING APPROACHES

Eser Çabuk

Supervisor: Prof. Dr. Uğurhan Akyüz

Middle East Technical University
Civil Engineering Department

cabukeser@gmail.com

Overview

1. Introduction
2. Building Model
3. Seismicity and Selected Ground Motions
4. Isolator Design and Nonlinear Models
5. Analysis
6. Results
7. Conclusions

1. Introduction

Seismic Isolation:

- Flexible layer that decouples the superstructure from the foundation
- More than 100 years of history with basic applications of sand, roller, rubber
- Modern applications include
  - Rubber type: Natural Rubber, High-Damping Rubber, Lead Rubber Bearings
  - Sliding type: Single, double or triple curved surface sliding isolators (Friction Pendulum)

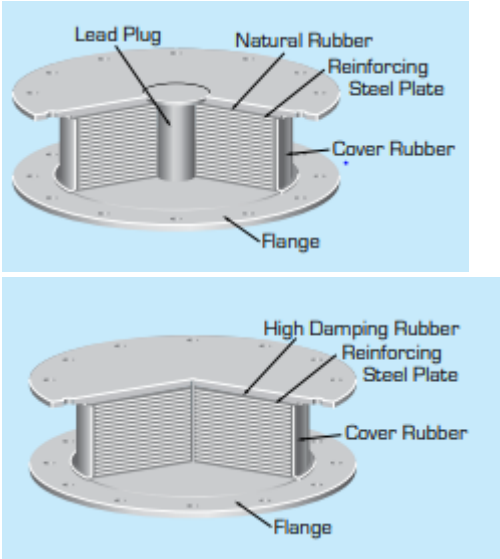

(Bridgestone Corporation)

Aim:

- To increase the natural vibration period to reduce spectral demands
- Add additional damping to the structure

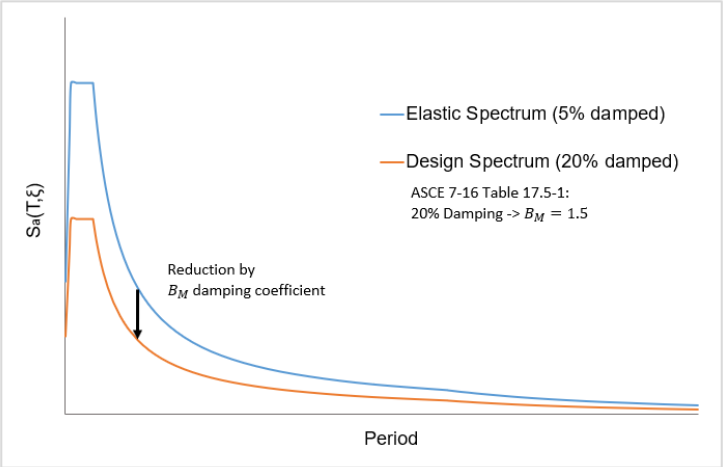

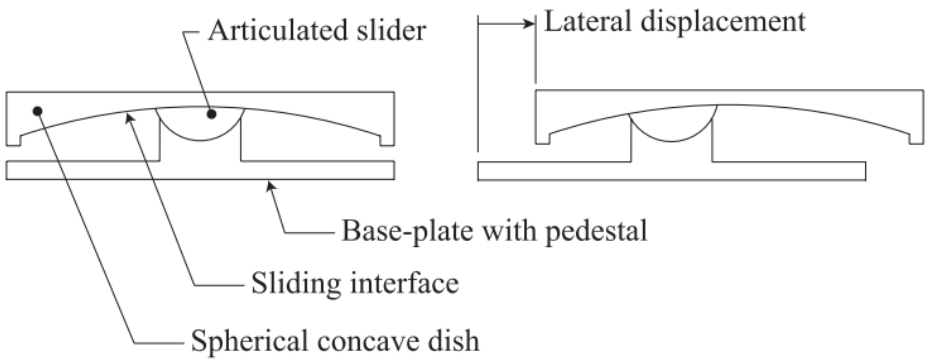

(Warn & Ryan, 2012)

1. Introduction

The seismic isolation has been in use in Turkey, especially for hospital buildings since 2013 to provide continuous service after the earthquakes. There are still lack of experience in architectural, engineering, production, testing and logistics aspects of a base isolated building design. (Erdik et al., 2018).

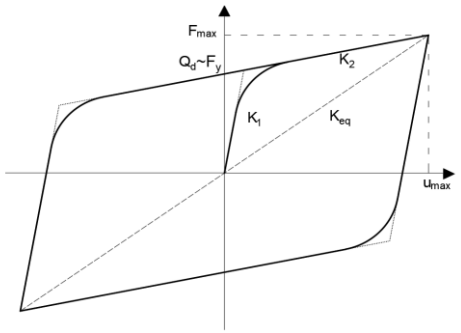

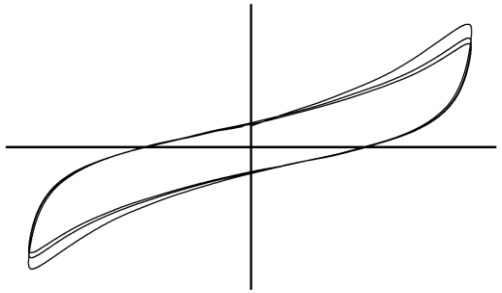

Problem Statement:

- Design according to ELFP, and performance check according to NLTH
- Different nonlinear models have been used in the design and the literature
  - Bilinear (Sharp and Smoothed) Models: Easy to implement in the analysis by the code requirements
  - Nonlinear Models: Better comprehension of dynamic isolator characteristics
- Literature and experience shows:
  - Difference in hysteretic characteristics might result in significant variations in the structural response

Aim:

- To assess the effect of modeling approach
- To highlight the advantages and drawbacks of different isolator models

on the response of EQ performance of 10-story T-shaped base isolated building according to TBDY2019

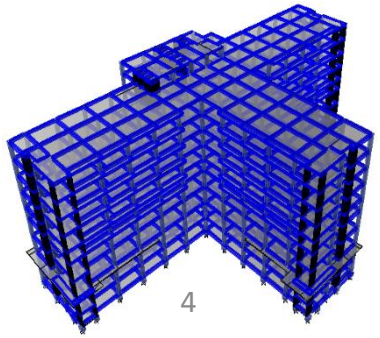

2. Building Model

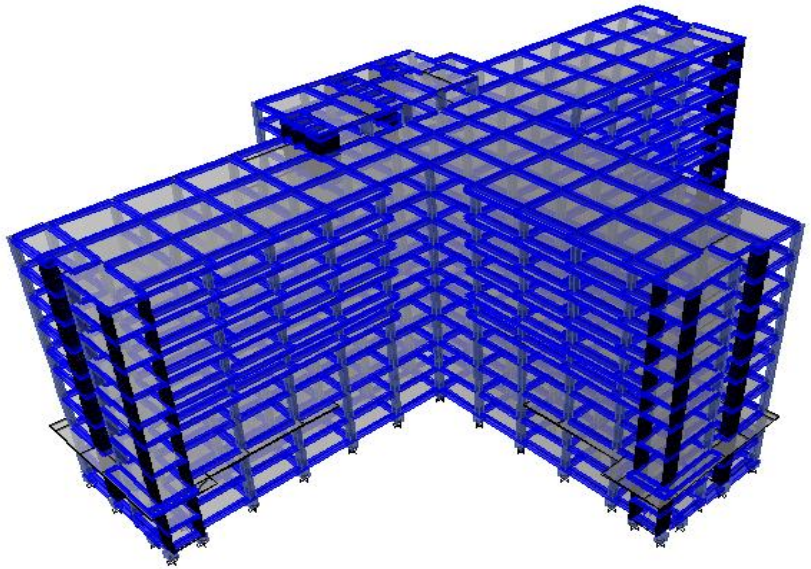

Building Information – ETABS Model	
# of floors	10
Building Type	Reinforced Concrete
Seismic Weight (G+0.3Q)	499727 kN
Plan Geometry	115x75 m
Aspect Ratio	2:1
# of iso	135

One of the 10 storey T-shaped blocks of a seismically isolated hospital in Turkey

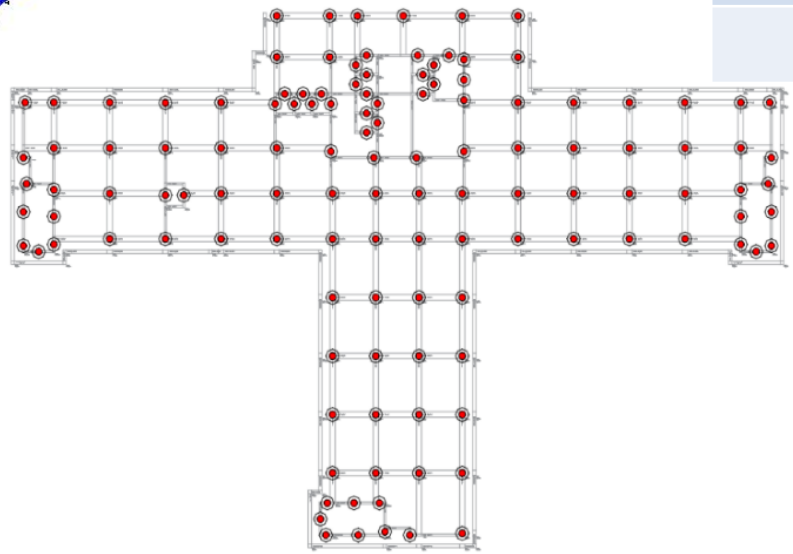

Isolator layout

Fixed Base Modes			
Mode	**Period**	**Mx**	**My**
1	1.912	0.4480	0.1148
2	1.860	0.1003	0.5920
3	1.693	0.1481	0.0019
4	0.559	0.0339	0.0320
5	0.547	0.0265	0.0475
6	0.490	0.026	0.0003

3. Seismicity and Selected Ground Motions

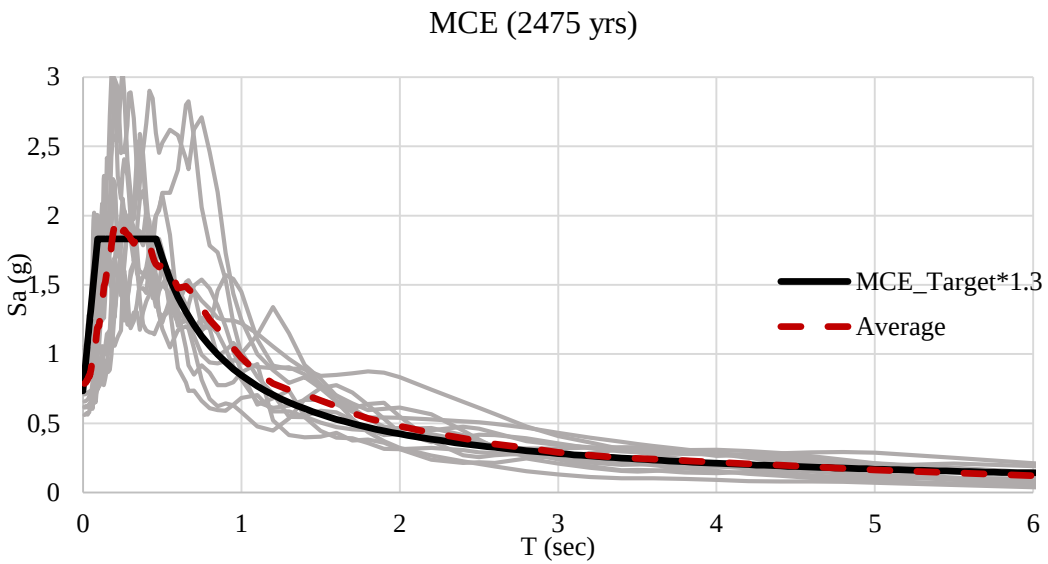

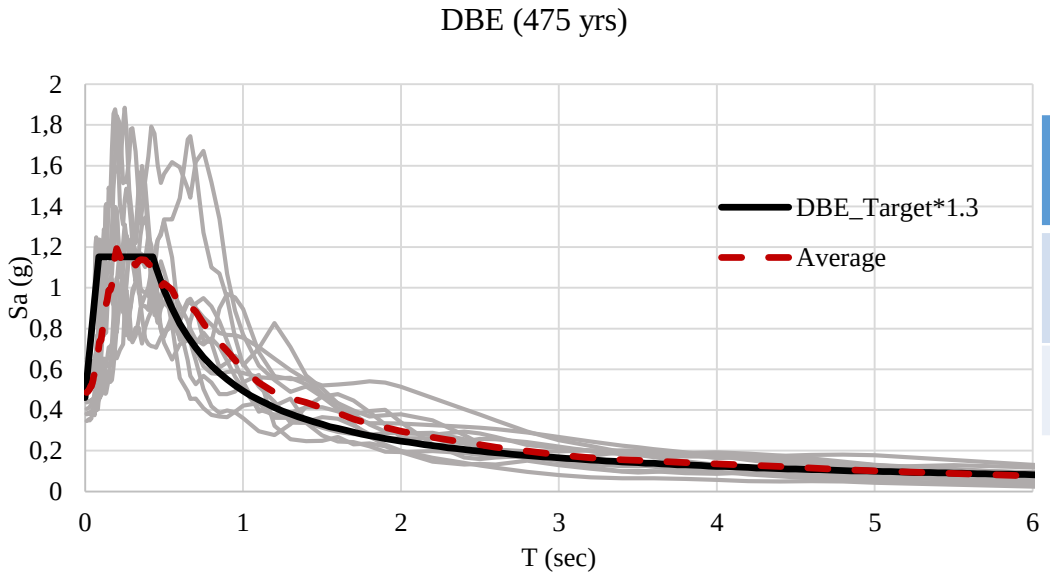

Seismicity of the region	
Vs30	350 m/s
Soil Class ZD	

Eq No	Record Seq. #	Tp-Pulse	Event	Year	Station	Rjb	Magnitude	Mechanism	Vs30 (m/s)	MCE_SF	DBE_SF
1	187	-	"Imperial Valley-06"	1979	"Parachute Test Site"	12.69	6.53	strike slip	348.7	3.892	2.404
2	316	4.389	"Westmorland"	1981	"Parachute Test Site"	16.54	5.9	strike slip	348.7	2.030	1.254
3	549	-	"Chalfant Valley-02"	1986	"Bishop - LADWP South St"	14.38	6.19	strike slip	303.5	2.826	1.746
4	558	-	"Chalfant Valley-02"	1986	"Zack Brothers Ranch"	6.44	6.19	strike slip	316.2	1.724	1.065
5	821	-	"Erzican_ Turkey"	1992	"Erzincan"	0	6.69	strike slip	352.1	1.125	0.695
6	850	-	"Landers"	1992	"Desert Hot Springs"	21.78	7.28	strike slip	359	3.530	2.180
7	1116	-	"Kobe_ Japan"	1995	"Shin-Osaka"	19.14	6.9	strike slip	256	2.487	1.536
8	1158	-	"Kocaeli_ Turkey"	1999	"Duzce"	13.6	7.51	strike slip	281.9	1.281	0.791
9	1605	-	"Duzce_ Turkey"	1999	"Duzce"	0	7.14	strike slip	281.9	0.947	0.585
10	2752	-	"Chi-Chi_ Taiwan-04"	1999	"CHY101"	21.62	6.2	strike slip	258.9	2.814	1.738
11	6893	-	"Darfield_ New Zealand"	2010	"DFHS"	11.86	7	strike slip	344	1.517	0.937

11 earthquake ground motions are retrieved from PEER Ground Motion Database: NGA-West2

4. Isolator Design and Nonlinear Models

Equivalent Lateral Force Procedure

HDRB UB: 1.45 LB: 0.9

Analysis Type		*MCE-LB*	*MCE-Nom*	*MCE-UB*	*DBE-LB*	*DBE-Nom*	*DBE-UB*
Seismic Weight (kN)	W			499727			
Effective Period (s)	T_M	2.942	2.765	2.208	2.510	2.326	1.774
Damping Ratio %	ξ	22%	22%	23%	24%	24%	24%
Total Effective Stiffness (kN/m)	K_M	232429	263189	412514	319363	371929	639180
Damping Scale Factor	η_M	0.610	0.606	0.594	0.587	0.587	0.535
Spectral Acc. (g)	$S_{ae}(T_M$	0.222	0.236	0.295	0.151	0.163	0.214
Max. Displ. (m)	D_M	0.378	0.353	0.276	0.181	0.167	0.116
Max. Disp. w/ Torsion (m)	D_{TM}	**0.416**	0.388	0.304	0.199	0.184	0.128
TBDY2018 Base Shear (V_m/W)		0.135	0.143	0.175	0.089	0.096	**0.114**
ASCE7-16 Base Shear (V_m/W)		0.143	0.152	0.186	0.095	0.102	**0.124**

FPS UB: 1.56 LB: 0.9

Analysis Type		*MCE-LB*	*MCE-Nom*	*MCE-UB*	*DBE-LB*	*DBE-Nom*	*DBE-UB*
Seismic Weight (kN)	W			499727			
Effective Period (s)	T_M	3.488	3.378	2.874	2.883	2.459	1.897
Damping Ratio %	ξ	21%	24%	30%	30%	30%	30%
Effective Stiffness (kN/m)	K_M	165289	176202	243426	241936	332616	558692
Damping Scale Factor	η_M	0.621	0.592	0.535	0.535	0.535	0.535
Spectral Acc. (g)	$S_{ae}(T_l$	0.187	0.193	0.227	0.132	0.154	0.200
Max. Displ. (m)	D_M	0.456	0.422	0.324	0.189	0.161	0.125
Max. Disp. w/ Torsion (m)	D_{TM}	**0.502**	0.464	0.356	0.208	0.177	0.137
TBDY2018 Base Shear (V_m/W)		0.116	0.114	0.121	0.070	0.083	**0.107**
ASCE7-16 Base Shear (V_m/W)		0.123	0.122	0.131	0.076	0.089	**0.116**

$$D_M = 1.3\left(\frac{g}{4\pi^2}\right)T_M^2\eta_M S_{ae}^{MCE}(T_M) \qquad V_M = \frac{S_{ae}^{MCE}(T_M)W\eta_M}{R}$$

4. Isolator Design and Nonlinear Models

High Damping Rubber Bearing (HDRB)

		Type 1	Type 2	Type 3	Type 4
# of isolator	#	57	36	25	17
Average Seismic Weight (kN)	G+0.3Qave	1649	4036	6099	6352
Maximum Earthquake Load (kN)	1.2G+Q+Emax	9000	12000	15000	17174
Minimum Eathquake Load (Tension) (kN)	0.9-Emax	580	737	915	958
Shear Modulus (kPa)	Gv	620	620	620	620
Vertical Rigidity (kN/m)	Kv	4283139	5058781	6166376	7402727
Outer Diameter (m)	Do (B)	0.9	1	1.1	1.2
Inner Diameter (m)	Di (BL)	0.02	0.055	0.055	0.055
Effective Area (m^2)	Ar	0.6359	0.7830	0.9480	1.1286
Inner Area (m^2)	Ai	0.000	0.002	0.002	0.002
Rubber layer thickness (m)	tr	0.006	0.0067	0.0074	0.008
Number of Layers	n	33	30	27	25
Tot. Rubber Height (m)	H	0.198	0.201	0.200	0.200
Tot. Iso. Height (m)	Ht	0.4108	0.4006	0.3902	0.3856
First Shape Factor	S1	36.7	35.3	35.3	35.8

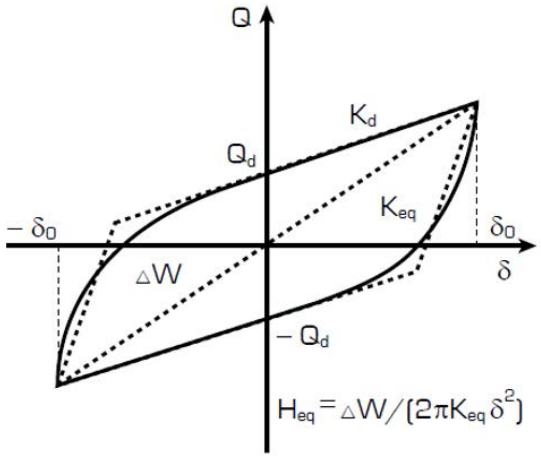

Ref: Bridgestone Isolation Product Line-up, 2017

- Max. Comp. Stress = 15 MPa
- Max Shear Strain = 200% (TBDY2019)
- Tensile Capacity = 1 MPa (Yang et al., 2015; Bridgestone)
- $\dfrac{\text{Tensile Stiffness}}{\text{Compression Stiffness}} = \dfrac{1}{30}$ (Pietra & Park, 2017)

MCE-Lower Bound Hysteretic Properties

	Type 1	Type 2	Type 3	Type 4
γ	1.469	1.447	1.455	1.454
D_m (m)	0.291	0.291	0.291	0.291
G_{eq} (kPa)	519	522	521	521
H_{eq} (ξ) %	0.232	0.232	0.232	0.232
u	0.392	0.393	0.392	0.392
K_{eq} (kN/m)	1500	1830	2224	2646
K_2 (kN/m)	913	1111	1351	1607
K_1 (kN/m)	8787	10659	12982	15440
Q_d (kN)	192.5	237.0	286.9	341.6
F_{max} (kN)	524.6	646.1	782.2	931.2

4. Isolator Design and Nonlinear Models

High Damping Rubber Bearing

DHI Model

(Kato et al., 2015; Masaki et al., 2017)

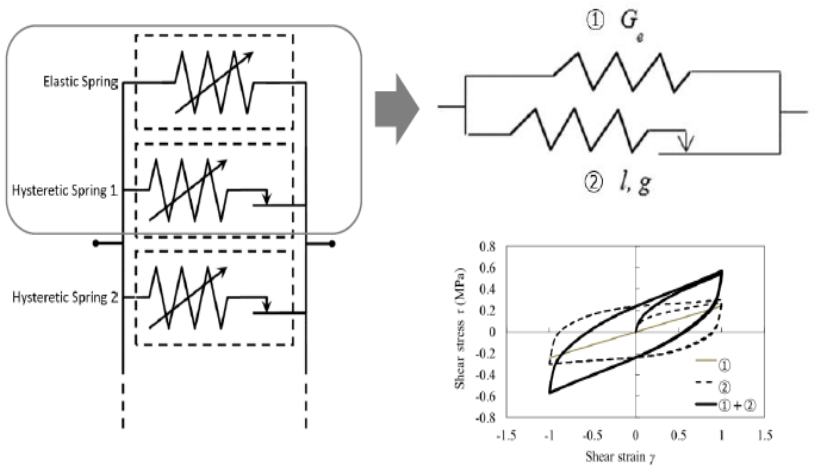

Ref: Bridgestone

$$\tau_x(\gamma_x,\gamma_y) = \Xi(t)G_e\gamma_x + \sum_i^n g_i \int_0^\Gamma e^{-(\Gamma-\Gamma')/l_i}\frac{d}{d\Gamma'}\left[\frac{1}{3}(\gamma_x'-\gamma_x)(\gamma_x'^2+\gamma_y'^2)+\gamma_x'\right]d\Gamma'$$

$$\tau_y(\gamma_x,\gamma_y) = \Xi(t)G_e\gamma_y + \sum_i^n g_i \int_0^\Gamma e^{-(\Gamma-\Gamma')/l_i}\frac{d}{d\Gamma'}\left[\frac{1}{3}(\gamma_y'-\gamma_y)(\gamma_x'^2+\gamma_y'^2)+\gamma_y'\right]d\Gamma'$$

$$\Xi(t) = \theta + (1-\theta)\exp\left(-\frac{\gamma_m(t)}{\gamma_d}\right)$$

- Can account for the bidirectional effects
- Stiffness increase when shear strain exceeds 200%

Smoothed BW

(Bouc, 1971; Wen,1976; Park et al., 1986)

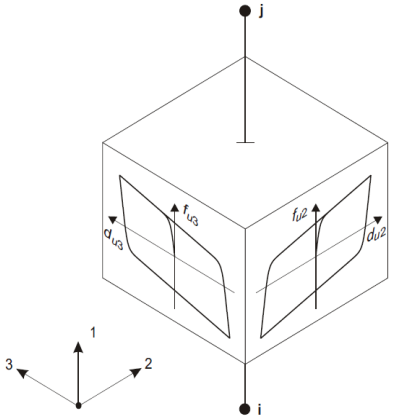

Ref: CSI Analysis Reference Manual, 2017

$$f_{u2} = ratio_2 k_2 d_{u2} + (1-ratio_2)yield_2 z_2$$

$$f_{u3} = ratio_3 k_3 d_{u3} + (1-ratio_3)yield_3 z_3$$

$$\begin{Bmatrix} \dot{z_2} \\ \dot{z_3} \end{Bmatrix} = \begin{bmatrix} 1-a_2z_2^2 & -a_3z_2z_3 \\ -a_2z_2z_3 & 1-a_3z_3^2 \end{bmatrix} \begin{Bmatrix} \frac{k_2}{yield_2}\dot{d_{u2}} \\ \frac{k_3}{yield_3}\dot{d_{u3}} \end{Bmatrix}$$

Sharp BL

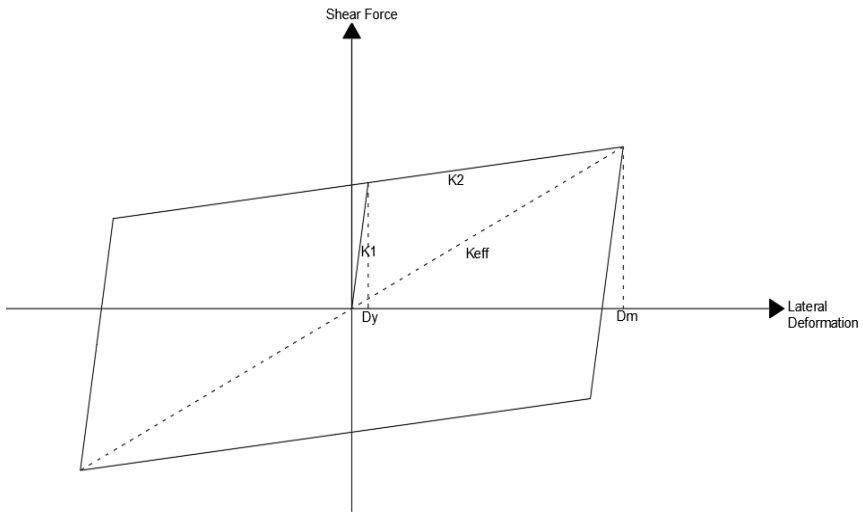

- Only unidirectional behavior
- Axial and lateral DOF's are not coupled

4. Isolator Design and Nonlinear Models

HDRB Models Input Parameters

DHI Model

Property	Nominal	UB	LB
Added Elastic Stiffness – G_e (MPa)	0.5257	0.8136	0.5262
Control Strength 1 - g_1 (MPa)	2.468	3.364	1.999
Control Strength 2 - g_2 (MPa)	0.3564	0.4858	0.2887
Control Strain 1 - l_1	0.03591	0.03591	0.03591
Control Strain 2 - l_2	0.5	0.5	0.5
Resistance Ratio - θ	0.4598	0.4598	0.4598
Damage Parameter – γ_d	0.4181	0.4181	0.4181

Smoothed BW

(Bouc, 1971; Wen,1976; Park et al., 1986)

		MCE-LB	DBE-Nom	DBE-UB
Type 1	keff2,3	1500	2599	4415
	k2,3	9127	15382	26310
	yield2,3	171	137	175
	ratio2,3	0.1		
Type 2	keff2,3	1830	3182	5399
	k2,3	11110	18839	32192
	yield2,3	209	167	214
	ratio2,3	0.1		
Type 3	keff2,3	2224	3861	6554
	k2,3	13512	22857	39073
	yield2,3	254	203	260
	ratio2,3	0.1		
Type 4	keff2,3	2646	4595	7800
	k2,3	16075	27202	46499
	yield2,3	302	242	310
	ratio2,3	0.1		

Sharp BL

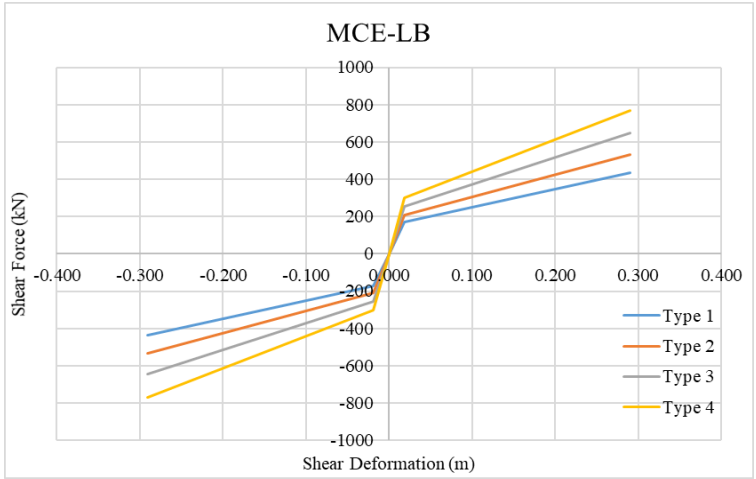

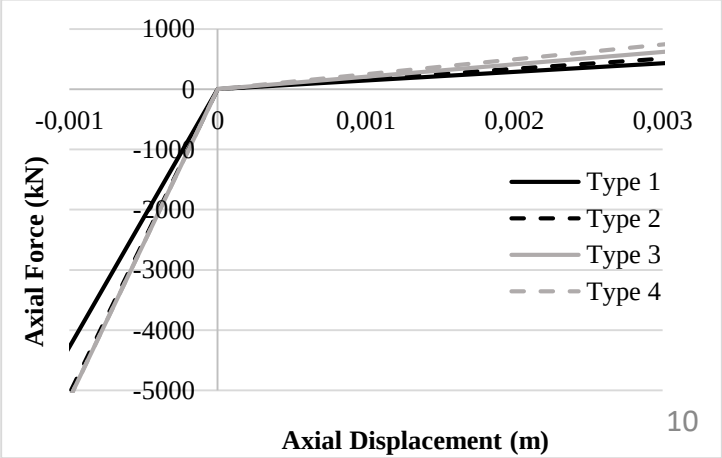

4. Isolator Design and Nonlinear Models

Friction Pendulum System (FPS)

Type	1	2	3
No. iso	68	42	25
G+0.3Q_ave (kN)	1839	5100	6365
1.2G+Q+E_max (kN)	10000	14000	17174
1.4G+1.6Q_max (kN)	8165	11013	12264
Friction coeff, μ	0.055		
Radius of Curv (m)	4.5		
Upper-Lower Bound	1.56-0.9		

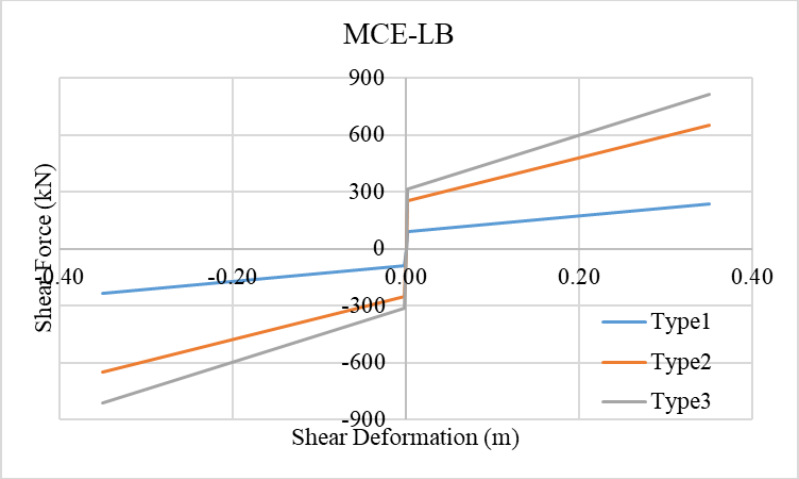

MCE-Level Total System Properties

		MCE-LB	MCE-Nom	MCE-UB
μ_e		0.0495	0.055	0.0858
R_C	m	4.5	4.5	4.5
D	m	0.351	0.325	0.249
$F_{y,total}$	kN	24736	27485	42877
$k_{2,total}$	kN/m	111050	111050	111050
$k_{1,total} = 100k_2$	kN/m	11105044	11105044	11105044
$k_{e,total}$	kN/m	181558	195747	283139
$F_{max,total}$	kN	63697	63522	70545
β_e	%	25%	28%	30%
T_{eff}	s	3.328	3.205	2.665
ω	rad	0.3005	0.3120	0.3752

4. Isolator Design and Nonlinear Models

Friction Pendulum System

FPI Model (Bouc, 1971; Wen,1976; Park et al., 1986, Zayas & Low, 1990)

$$f_{u1} = P = \begin{cases} \boldsymbol{k_1} d_{u1} & if\ d_{u1} < 0 \\ 0 & otherwise \end{cases}$$

$$f_{u2,3} = \underset{friction}{f_{u2,3f}} + \underset{pendulum}{f_{u2,3p}}$$

$$f_{u2,3f} = -P\mu_{2,3} z_{2,3}$$

$$f_{u2,3p} = -P\frac{d_{u2,3}}{\boldsymbol{radius_{2,3}}}$$

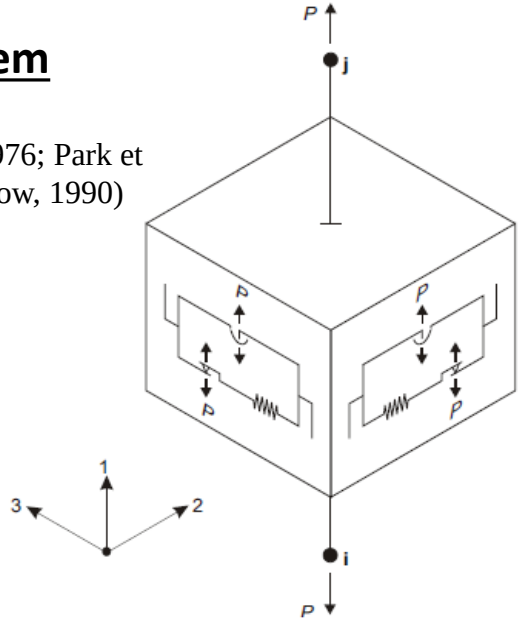

Ref: CSI Analysis Reference Manual, 2017

- High axial load dependency on friction and pendulum behavior

Where

$$\mu_{2,3} = \boldsymbol{fast_{2,3}} - (\boldsymbol{fast_{2,3}} - \boldsymbol{slow_{2,3}})e^{-rv}$$

$$v = \sqrt{\dot{d}_{u2,3}^2 + \dot{d}_{u3,2}^2}$$

$$r = \frac{\boldsymbol{rate_{2,3}}\,\dot{d}_{u2,3}^2 + \boldsymbol{rate_{3,2}}\dot{d}_{u3,2}^2}{v^2}$$

BL Model

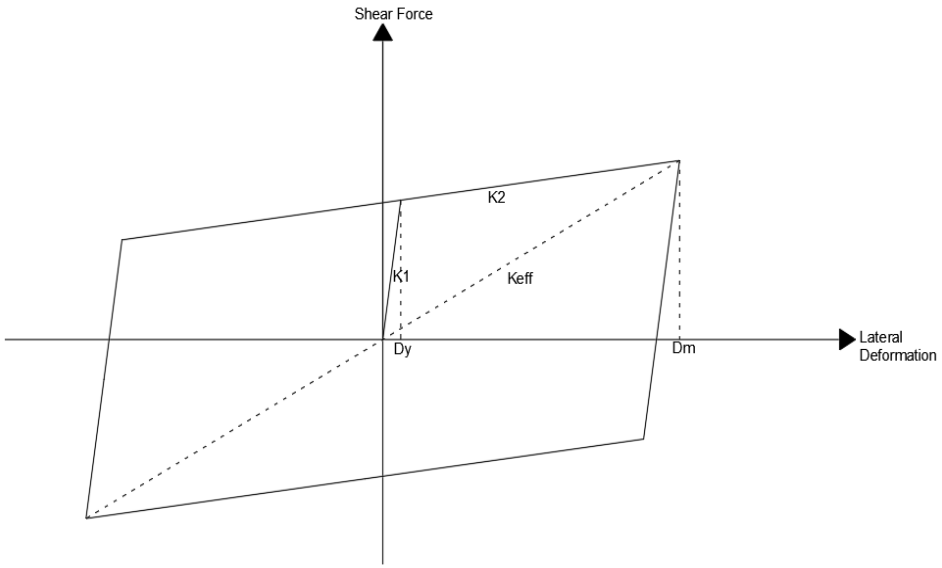

- Only unidirectional behavior
- Axial and lateral DOF's are not coupled

4. Isolator Design and Nonlinear Models

Friction Pendulum System Input Parameters

FPI Model

	Type 1	*Type 2*	*Type 3*
k2,3	40872	113327	141448
slow2,3	0.0396	0.0396	0.0396
fast2,3	0.0495	0.0495	0.0495
rate2,3		1	
radius2,3		4.5	

BL Model

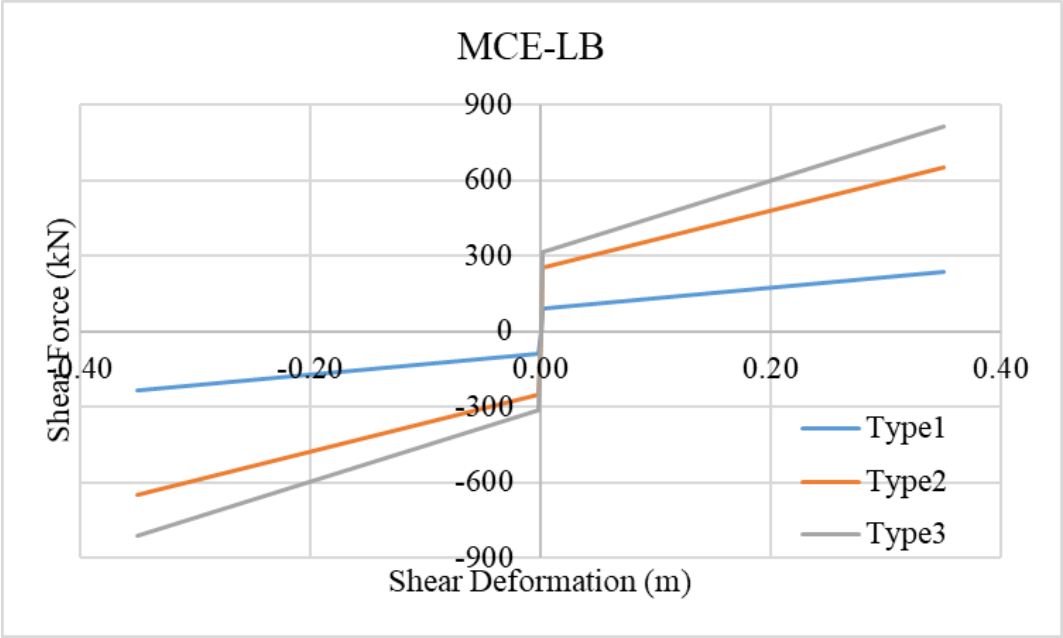

5. Analysis

Nonlinear Modal Time History (Fast Nonlinear) Analysis

Dynamic Equilibrium Equation

$$\mathbf{M}\ddot{\boldsymbol{u}}(t) + \boldsymbol{C}\dot{\boldsymbol{u}}(t) + \boldsymbol{K}_L\boldsymbol{u}(t) + \boldsymbol{R}(t)_{NL} = \boldsymbol{R}(t)$$

In some cases, the model become unstable without the stiffness of nonlinear elements,

$$\mathbf{M}\ddot{\boldsymbol{u}}(t) + \boldsymbol{C}\dot{\boldsymbol{u}}(t) + (\boldsymbol{K}_L + \boldsymbol{K}_{NL})\boldsymbol{u}(t) = \boldsymbol{R}(t) - \boldsymbol{R}_{NL}(t) + \boldsymbol{K}_{NL}\boldsymbol{u}(t)$$

$$\mathbf{M}\ddot{\boldsymbol{u}}(t) + \boldsymbol{C}\dot{\boldsymbol{u}}(t) + \boldsymbol{K}\boldsymbol{u}(t) = \overline{\boldsymbol{R}}(t)$$

- Ritz Vector solution
- 500 modes included

- Seismic weight is applied for initial condition
- Total of 22 load case (two pairs for each ground motion)
- Peak response of each pair were obtained

6. Results

Maximum Isolation Displacements

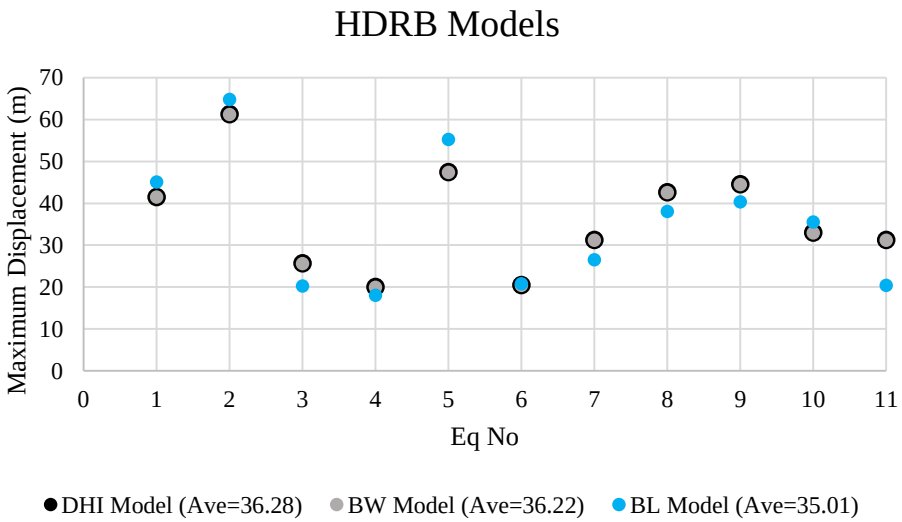

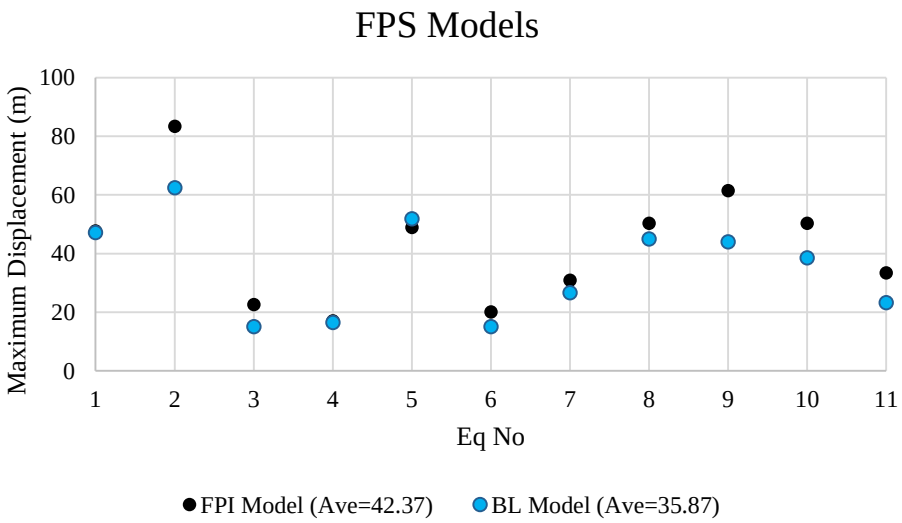

- Results from MCE-LB analysis
- Very similar response for DHI, BW and FPI model, and closer to the results of ELFP
- Response can be underestimated or overestimated by the bilinear models when ground motions are assessed separately
- The displacements are highly dependent on ground motion characteristics

6. Results

Structural Forces

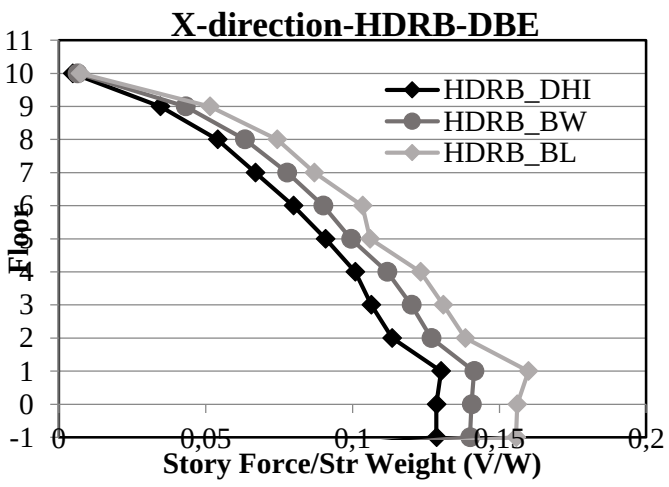

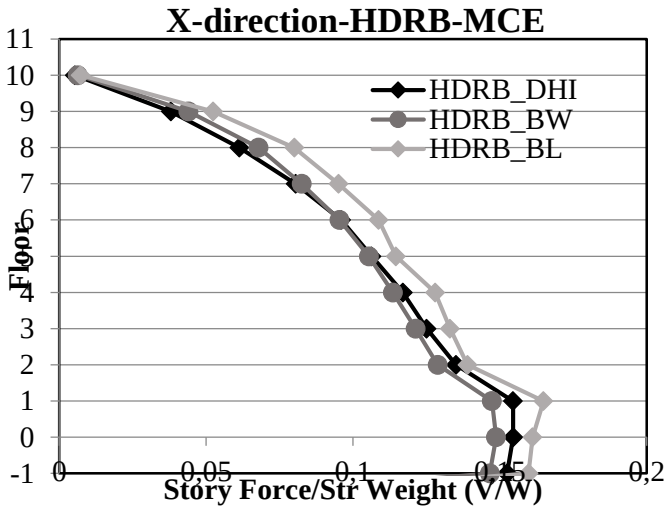

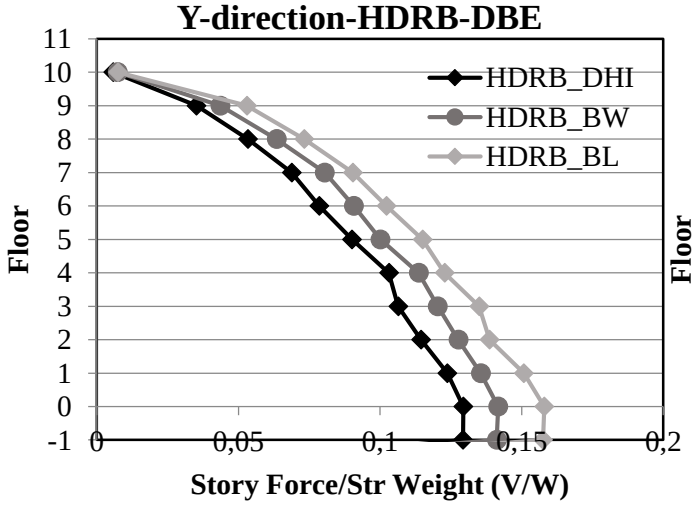

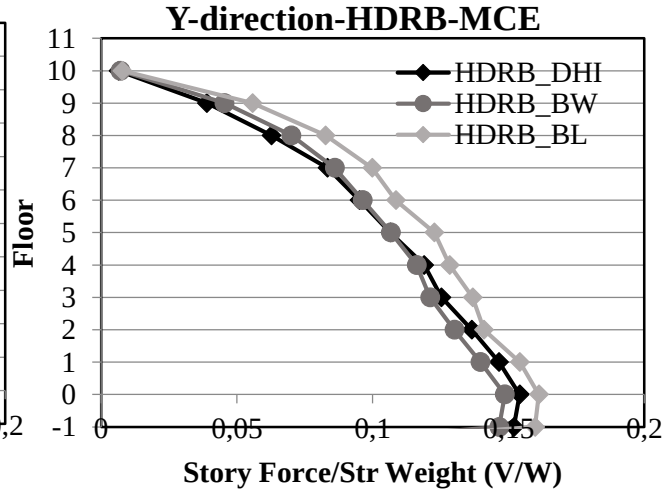

- Results from DBE-UB analysis
- Overestimation of the forces when sharp BL model are used
- Significant amplification on the First floor in X direction especially for earthquakes with pulse-like behavior and high scale factors
- The difference between each model is more insignificant in MCE

Vx/W Str. Weight=499727		TBDY2019-Base Shear	ASCE7-16 Superstr Force	TBDY Difference	ASCE Difference
DHI	0.130	0.126	0.134	3.5%	-2.9%
BW	0.141			12.5%	5.5%
BL	0.160			27.1%	19.3%

Vy/W Str. Weight=499727		TBDY2019 Base Shear	ASCE7-16 Superstr Force	TBDY Difference	ASCE Difference
DHI	0.124	0.126	0.134	-1.6%	-7.7%
BW	0.136			7.8%	1.1%
BL	0.151			19.9%	12.5%

6. Results

Structural Forces

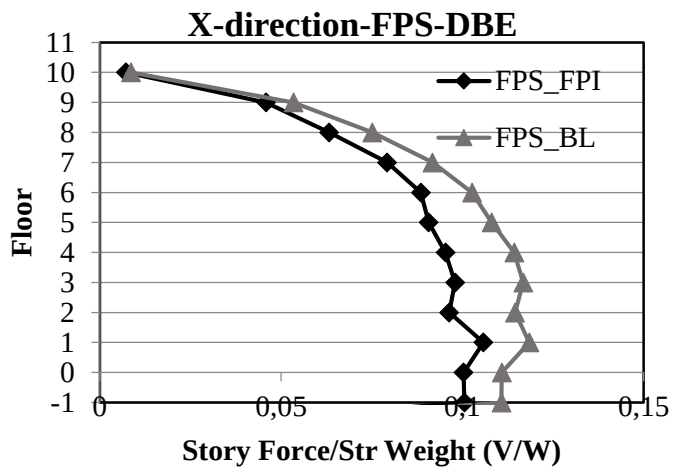

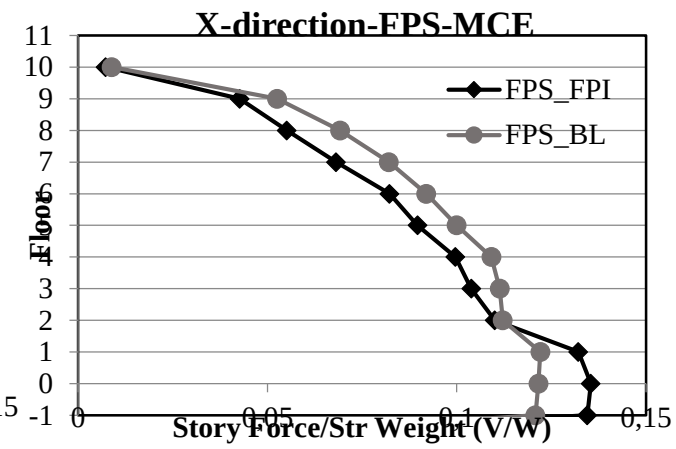

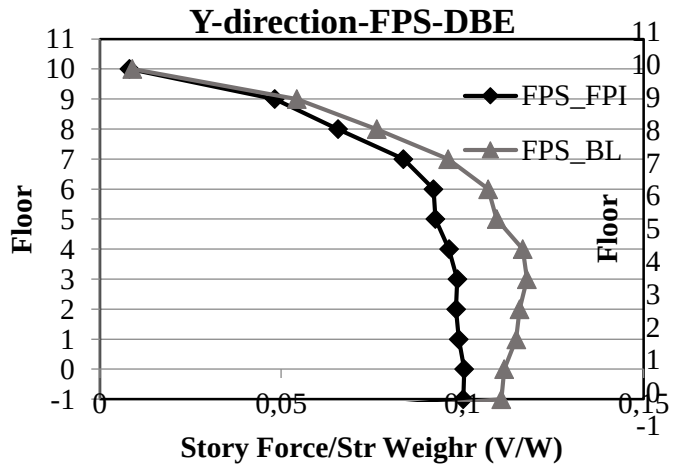

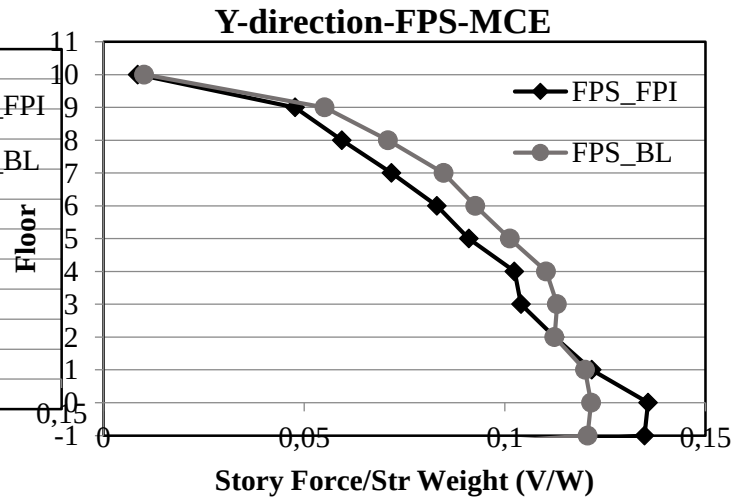

- Results from DBE-UB analysis
- Overestimation of the forces when sharp BL model are used
- Significant amplification on the First floor in X direction especially for earthquake with pulse-like behavior
- The difference between each model is more insignificant in MCE

Vx/W Str. Weight=499727		TBDY2019-Base Shear	ASCE7-16 Superstr Force	TBDY Difference	ASCE Difference
FPI	0.106	0.107	0.116	-1.2%	-8.8%
BL	0.118			10.7%	2.1%

Vy/W Str. Weight=499727		TBDY2019-Base Shear	ASCE7-16 Superstr Force	TBDY Difference	ASCE Difference
FPI	0.099	0.107	0.116	-7.5%	-14.7%
BL	0.115			7.3%	-1.0%

6. Results

Floor Accelerations

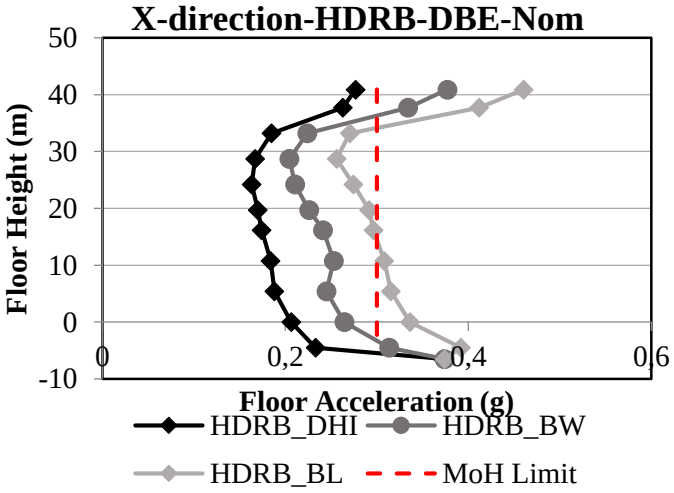

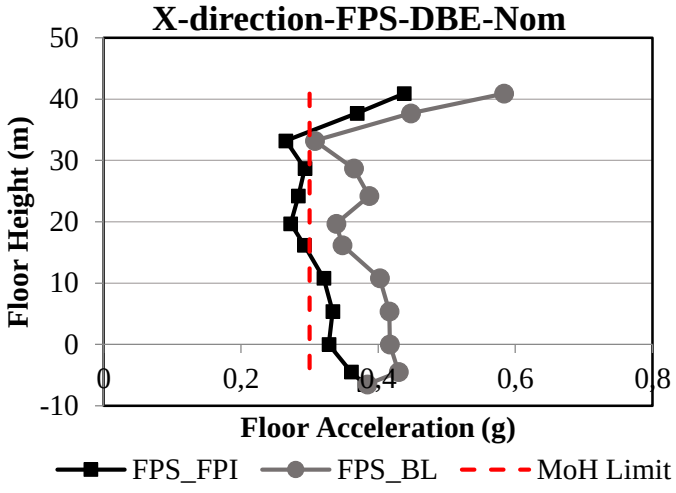

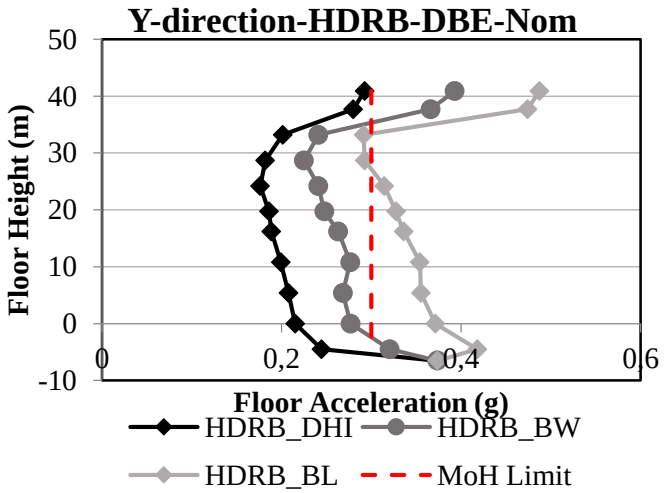

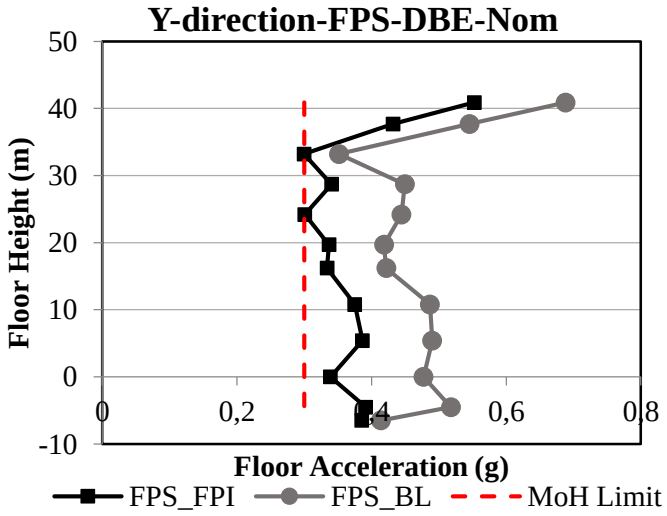

- Results from DBE-Nom analysis
- Overestimation of the response when bilinear models are used
- Acc. amplification on the isolation floor for the sharp BL (elevation -4.5)
- The sharp BL model cannot satisfy the target performance
- The DBE properties and rotational behavior of the structure has also significant effects on the response

6. Results

Inter-Storey Drifts

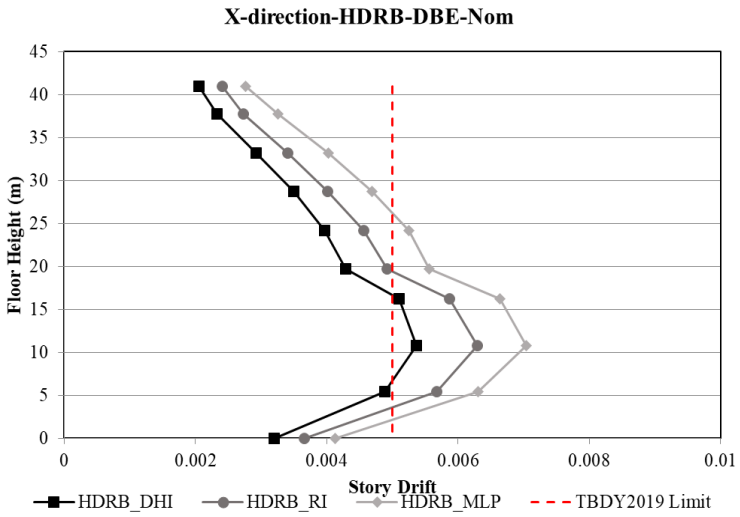

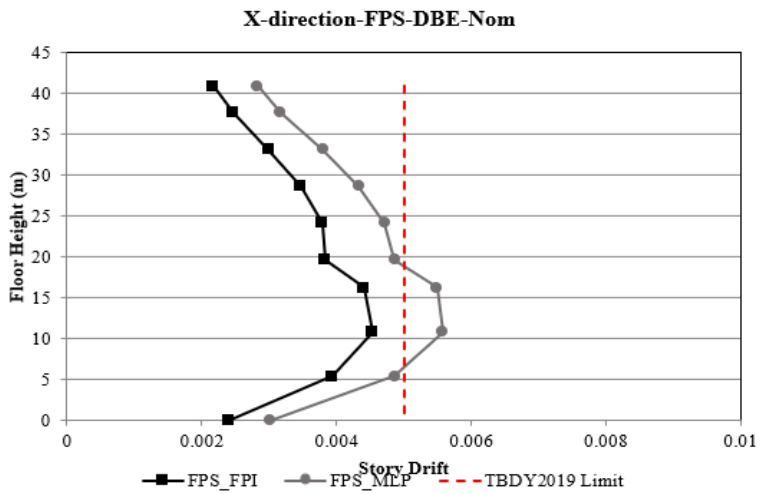

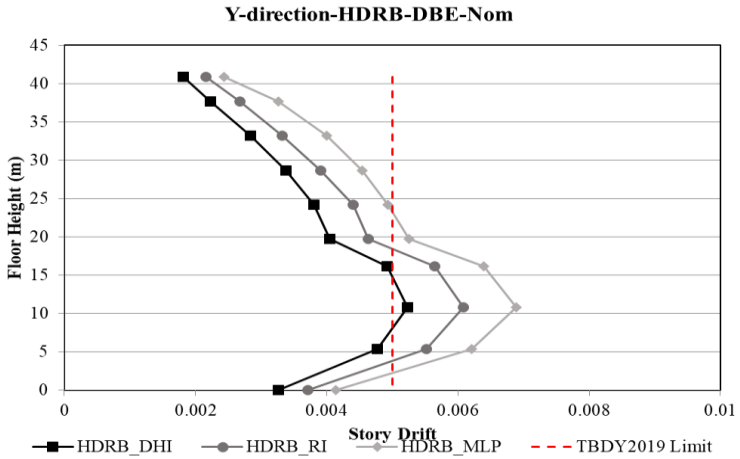

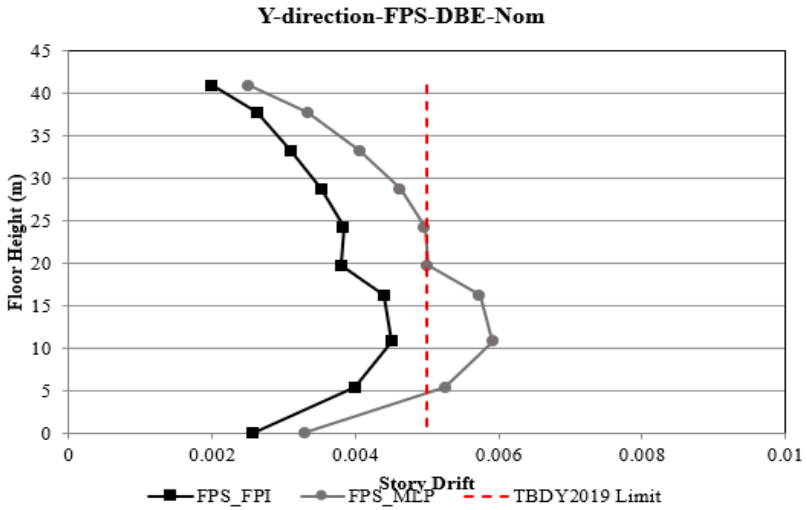

- Results from DBE-Nom analysis
- Overestimation of the response when bilinear models are used
- The target performance is not satisfied especially on the lower floors

6. Results

Isolator Hysteretic Curves

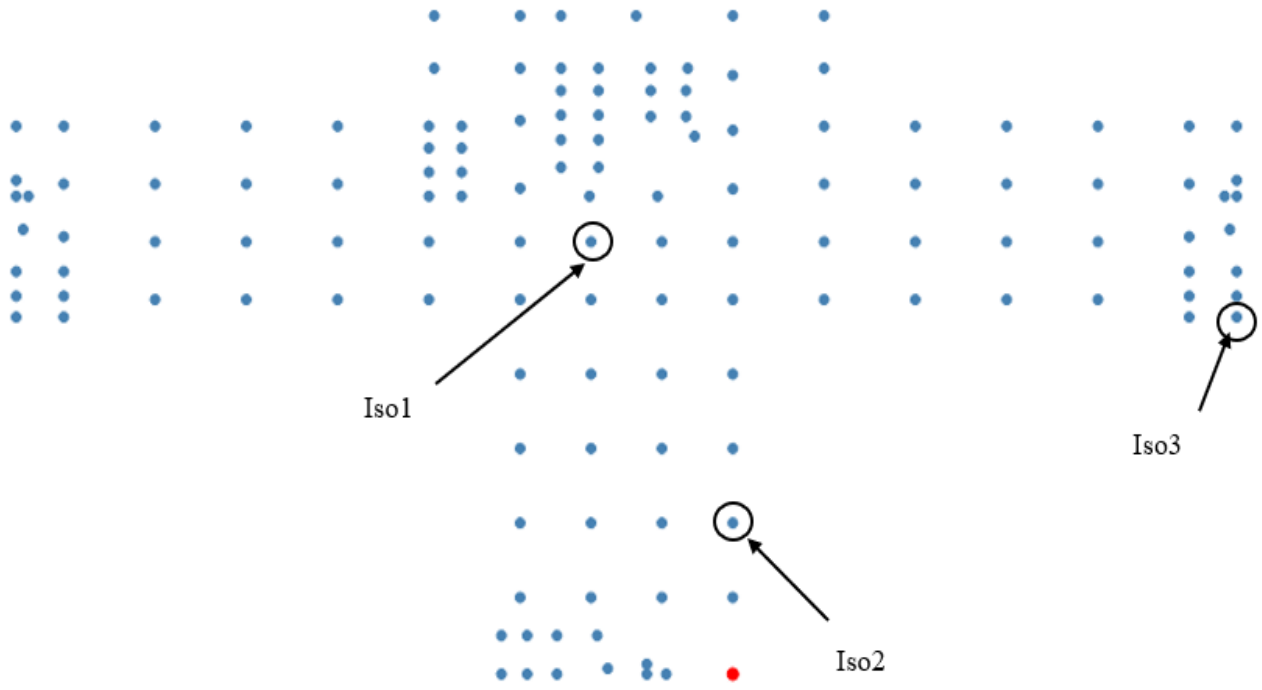

- Results from MCE-LB analysis
- Three locations from the building
  - Iso 1 - Middle
  - Iso 2 - Edge
  - Iso 3 – Corner/Shear Wall

6. Results

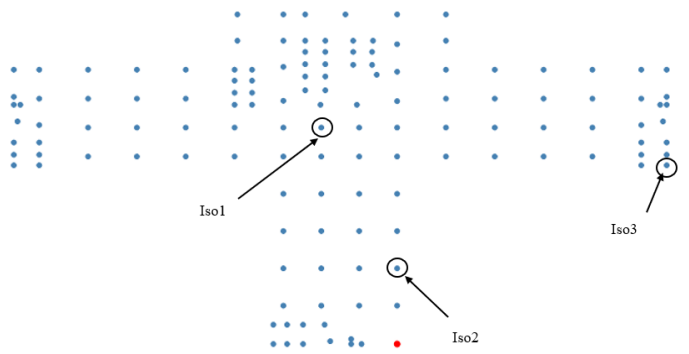

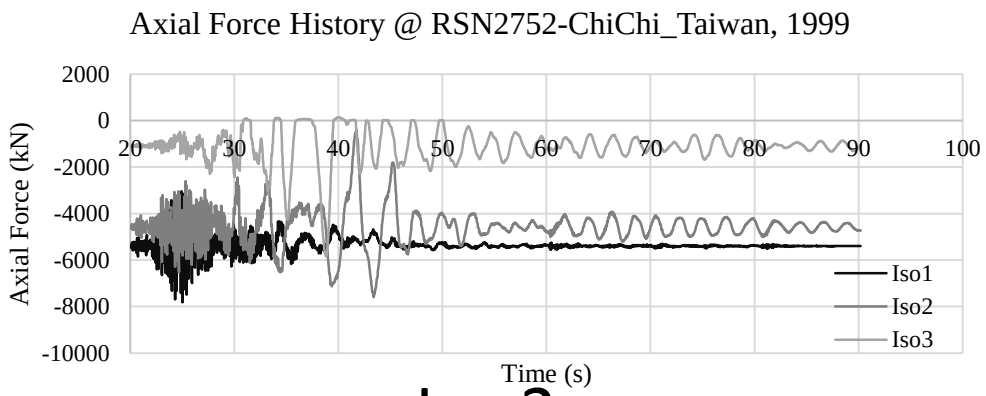

Iso 1

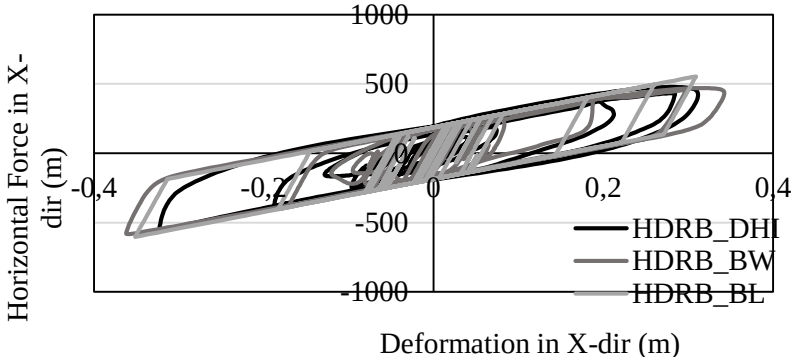

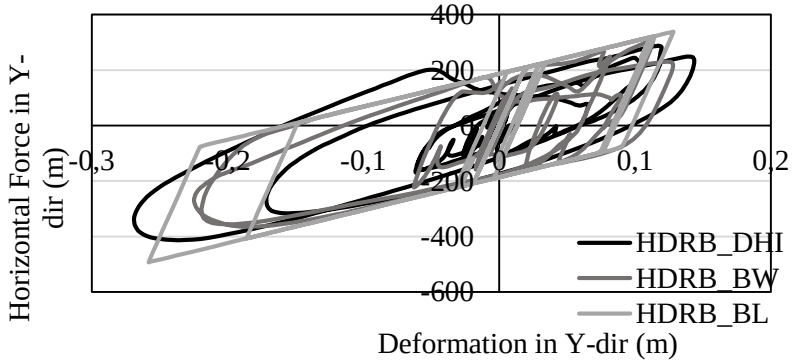

Iso 2

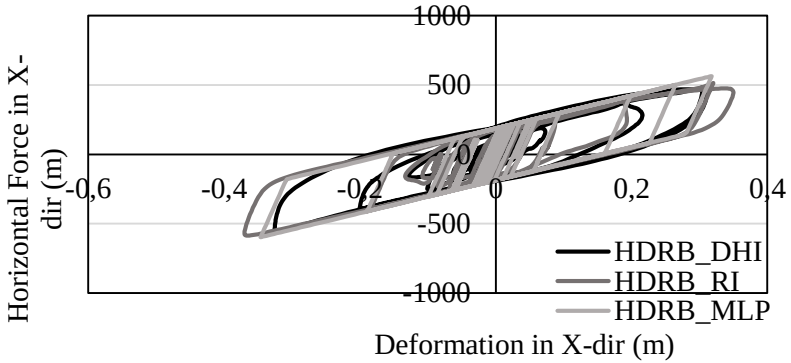

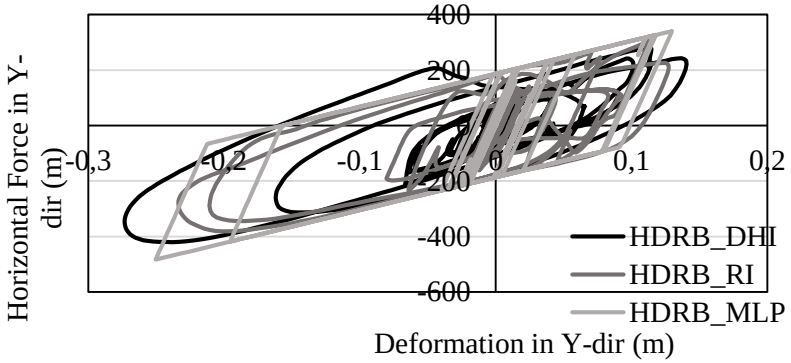

Iso 3

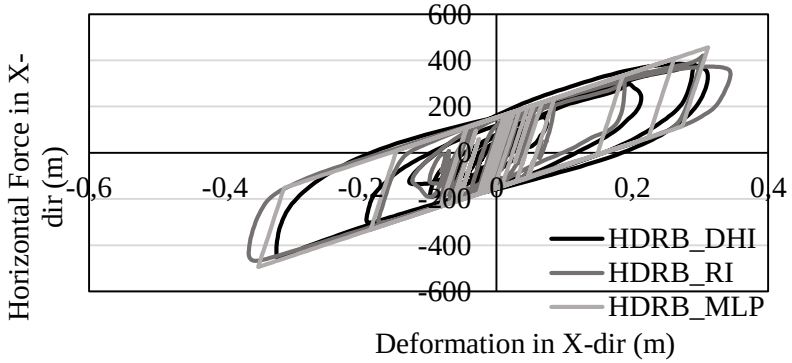

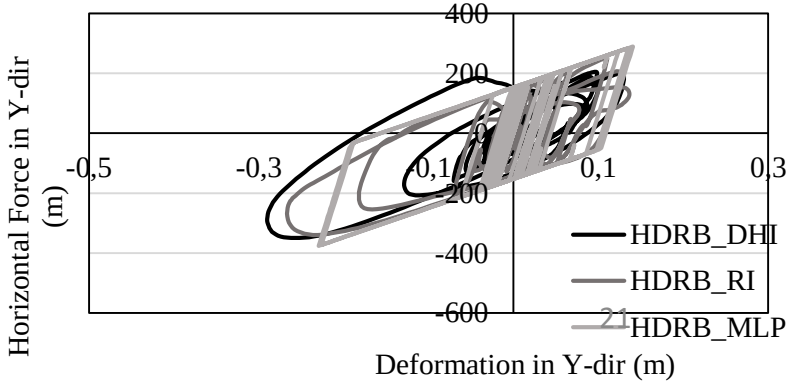

6. Results

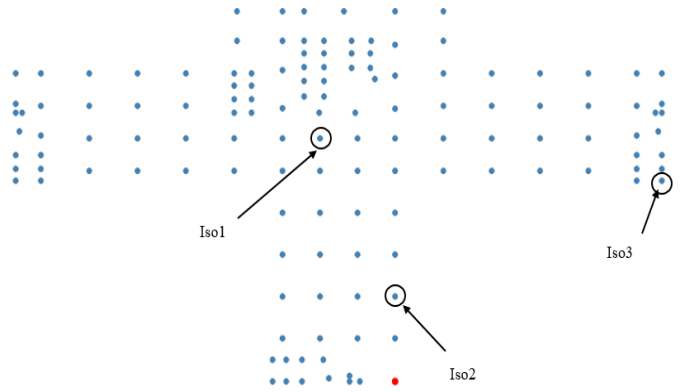

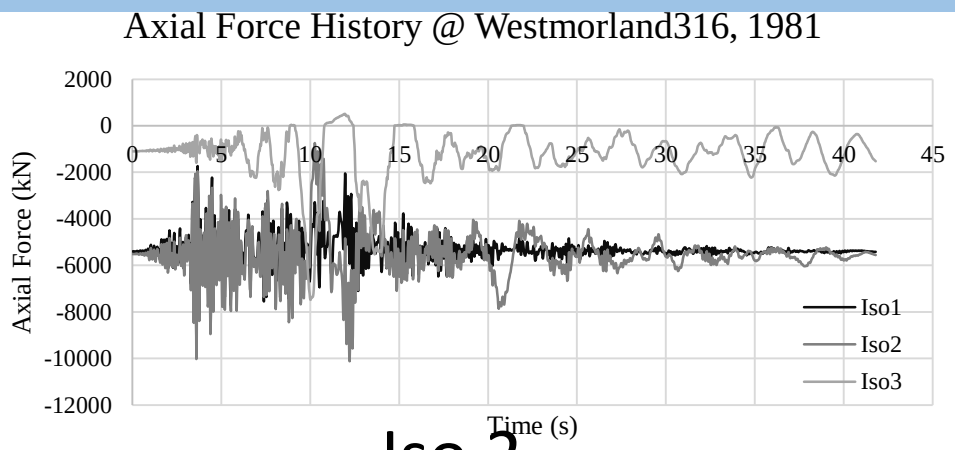

Iso 1

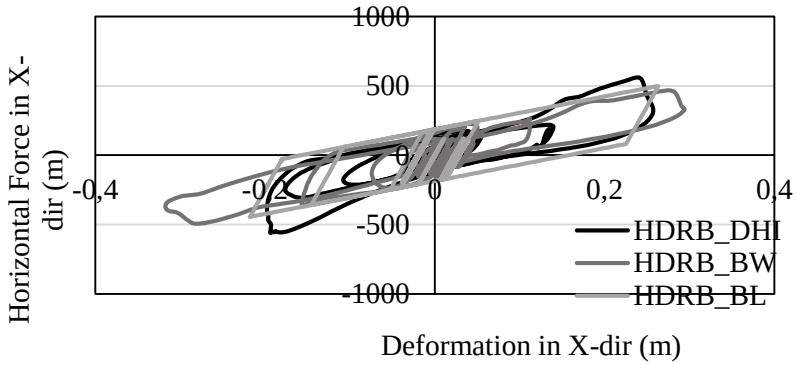

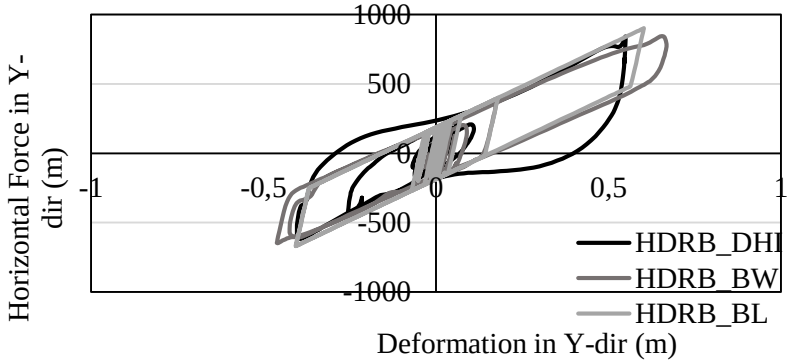

Iso 2

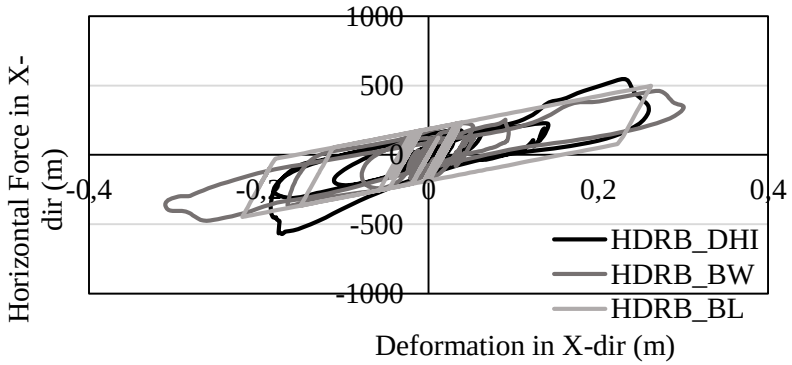

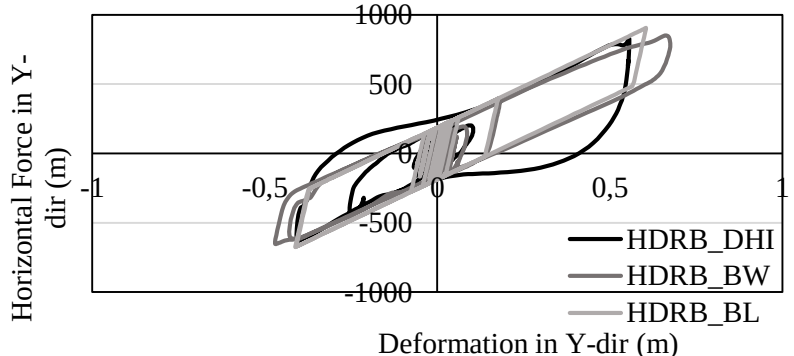

Iso 3

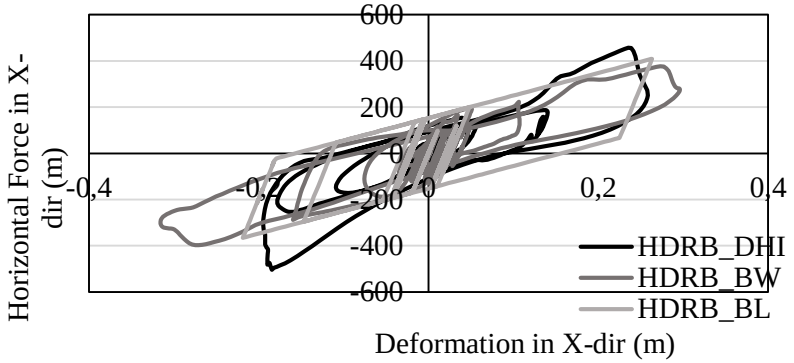

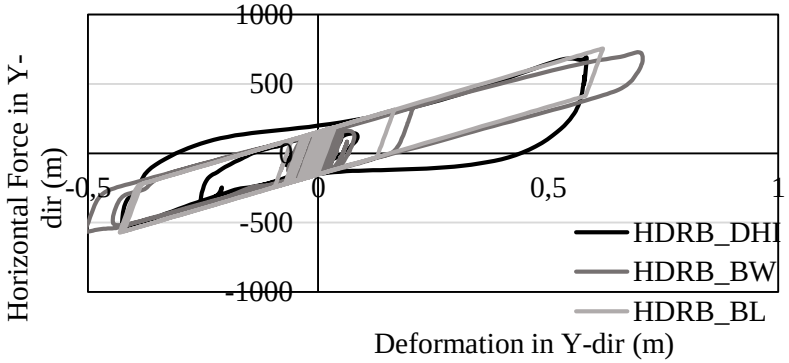

6. Results

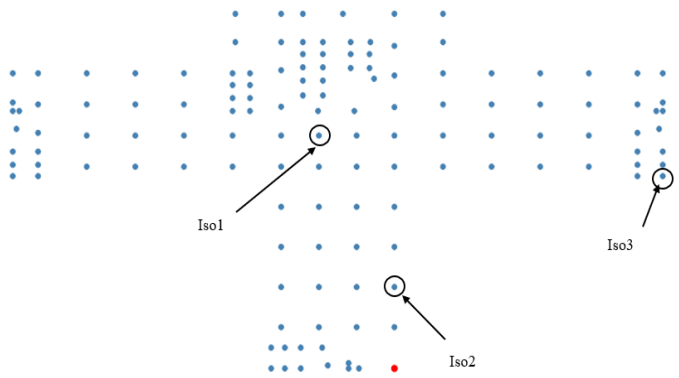

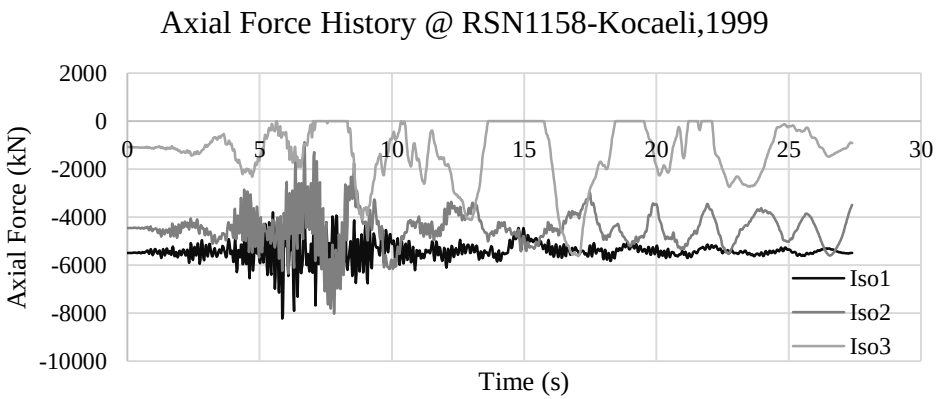

Iso 1

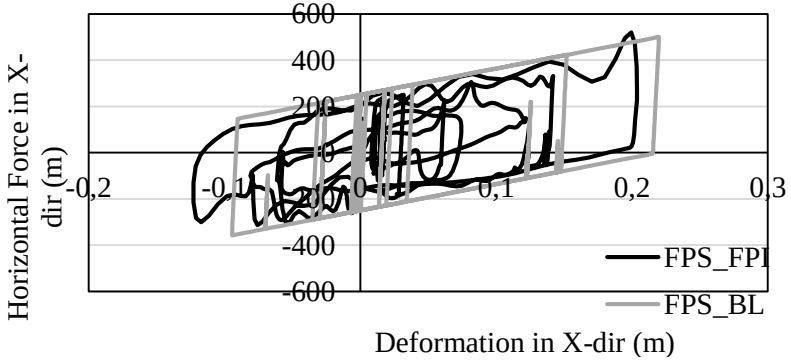

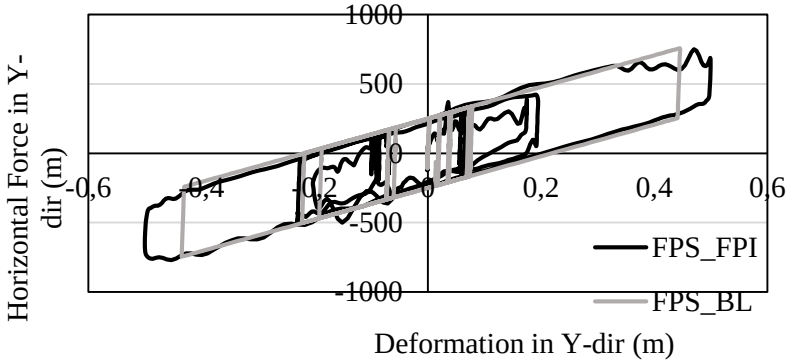

Iso 2

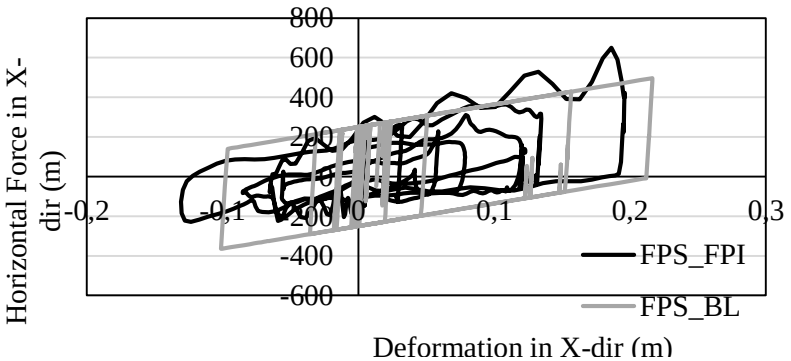

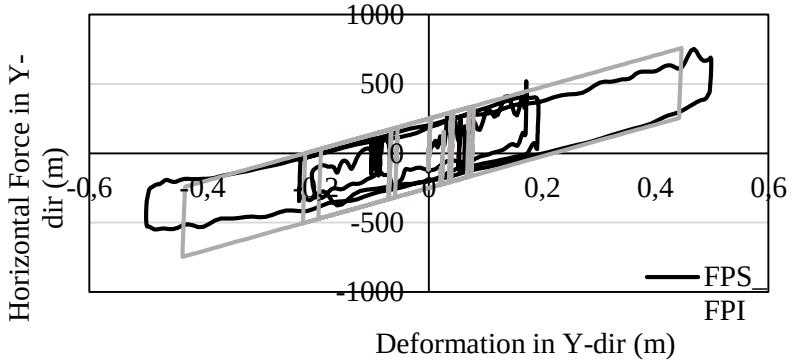

Iso 3

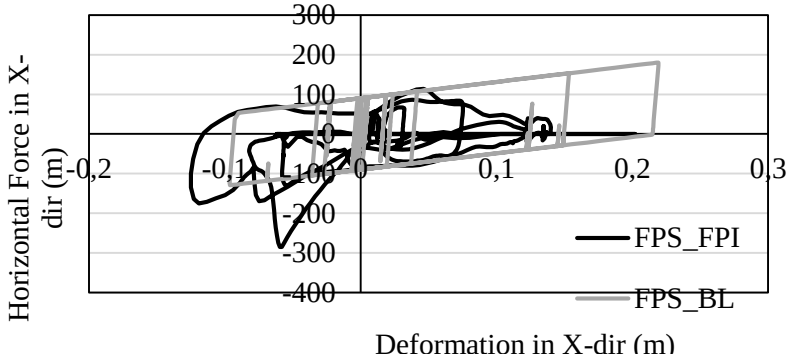

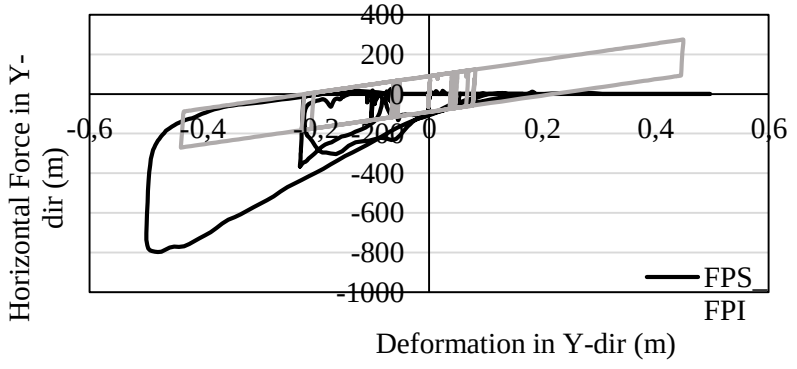

6. Results

Uplift Behavior

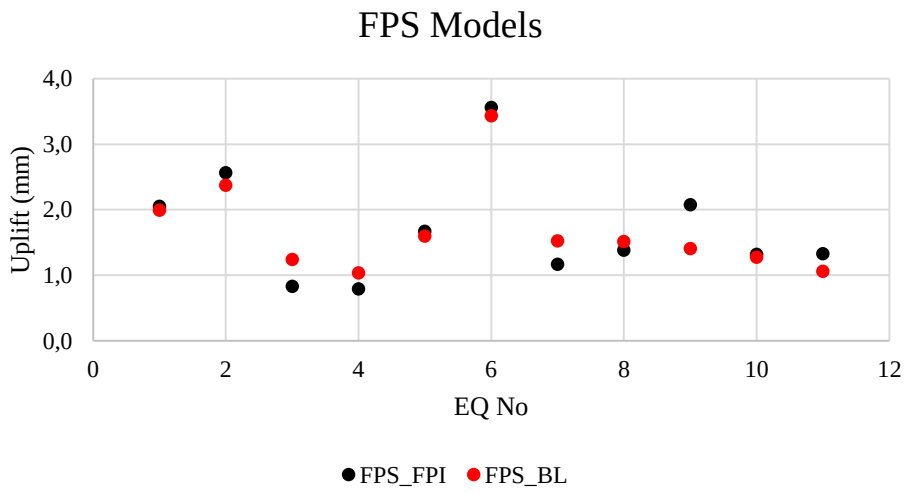

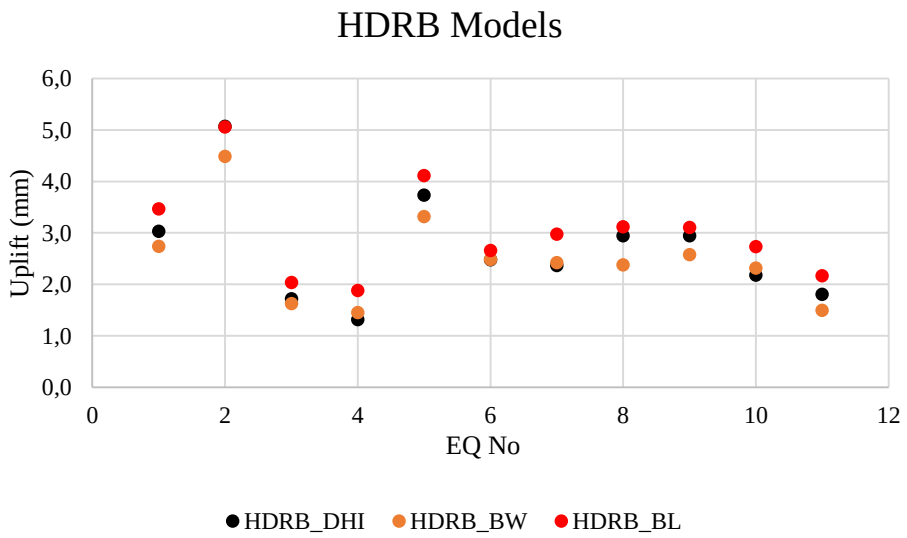

- Results from MCE-LB analysis
- Uplifts of FPS are in the range of 2-3 mm, however in Kocaeli1158 ground motion uplift durations of 1-2 sec is observed which may induce damage (Fenz, 2008)
- Uplift disp. of HDRB's are under 5% tensile strain, no cavitation damage expected (Yang et al. 2010)
- The sharp BL model overpredicts tensile stresses, exceeding 1 MPa limit for Type 4 isolators

	Maximum Tensile Stresses (kPa)											
	DHI Types				BW Types				BL Types			
	1	2	3	4	1	2	3	4	1	2	3	4
Ave	560	682	644	941	519	633	607	920	566	744	697	1110

7. Conclusions

- The isolator displacements can be overestimated or underestimated by the bilinear models. On average, the sharp BL model underestimates the displacements
- Superstructural forces, accelerations, drifts and uplift response are overestimated when the bilinear models are used.
- The sharp bilinear model could only capture the general hysteresis behavior of the HDRB isolators.
- Engineers should carefully assess each model's capabilities and the possible structural response before conducting analysis and design

Future Work:

- Modification of the bilinear model to capture hysteretic response
- Parametric study on the bilinear models with various ground motions, normalized isolator characteristic strength and stiffnesses to investigate higher response

Thank you!

7. References

- Fenz, D. M. (2008). DEVELOPMENT, IMPLEMENTATION AND VERIFICATION OF DYNAMIC ANALYSIS MODELS FOR MULTI-SPHERICAL SLIDING BEARINGS. State University of New York.
- Yang, Q. R., Liu, W. G., He, W. F., & Feng, D. M. (2010). Tensile Stiffness and Deformation Model of Rubber Isolators in Tension and Tension-Shear States. Journal of Engineering Mechanics, 136(4), 429–437.
- Pietra, D., & Park, A. R. L. (2017). Behaviour and Modelling of Lead-Rubber Bearings Subjected To Tensile Actions. 16th World Conference on Earthquake, 16WCEE.
- Erdik, M., Ülker, Ö., Şadan, B., & Tüzün, C. (2018). Seismic isolation code developments and significant applications in Turkey. Soil Dynamics and Earthquake Engineering, 115, 413–437.
- Disaster and Emergency Management Presidency, T. M. of the I. (2018). Türkiye Bina Deprem Yönetmeliği 2019 (Vol. 30364, Issue 1).
- Kato, H., Mori, T., Murota, N., & Kikuchi, M. (2015). Analytical Model for Elastoplastic and Creep-Like Behavior of High-Damping Rubber Bearings. Journal of Structural Engineering, 141(9), 04014213.
- Masaki, N., Mori, T., Murota, N., & Kasai, K. (2017). Validation of Hysteresis Model of Deformation-History Integral Type for High Damping Rubber Bearings
- Bouc, R. (1971). Modele mathematique d’hysteresis. Acustica, 24(1), 16–25.
- Wen, Y.-K. (1976). Method for Random Vibration of Hysteretic Systems. Journal of the Engineering Mechanics Division, 102(2), 249–263.
- Park, Y. J., Wen, Y. K., & Ang, A. H.-S. (1986). Random vibration of hysteretic systems under bi-directional ground motions. Earthquake Engineering & Structural Dynamics, 14(4), 543–557
- Zayas, V. A., Low, S. S., & Mahin, S. A. (1990). A Simple Pendulum Technique for Achieving Seismic Isolation. Earthquake Spectra, 6(2), 317–333.

6. Appendix

Floor Accelerations

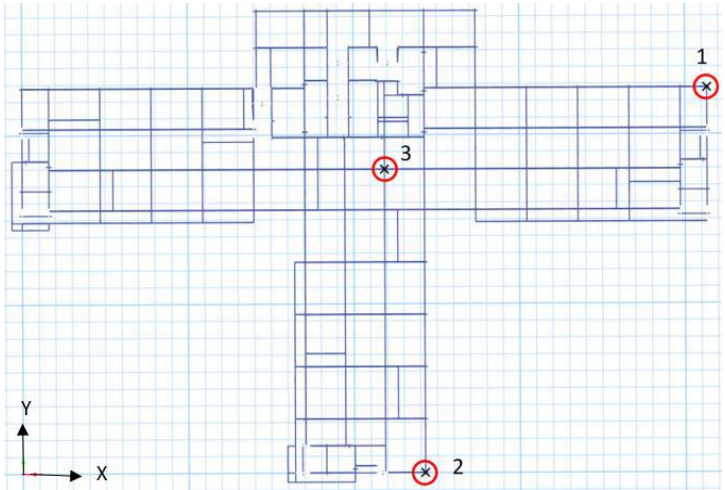
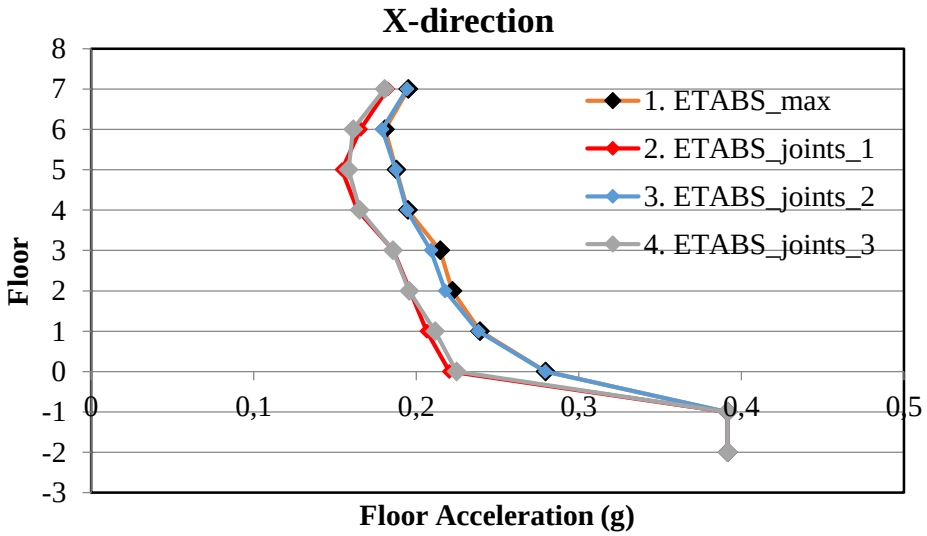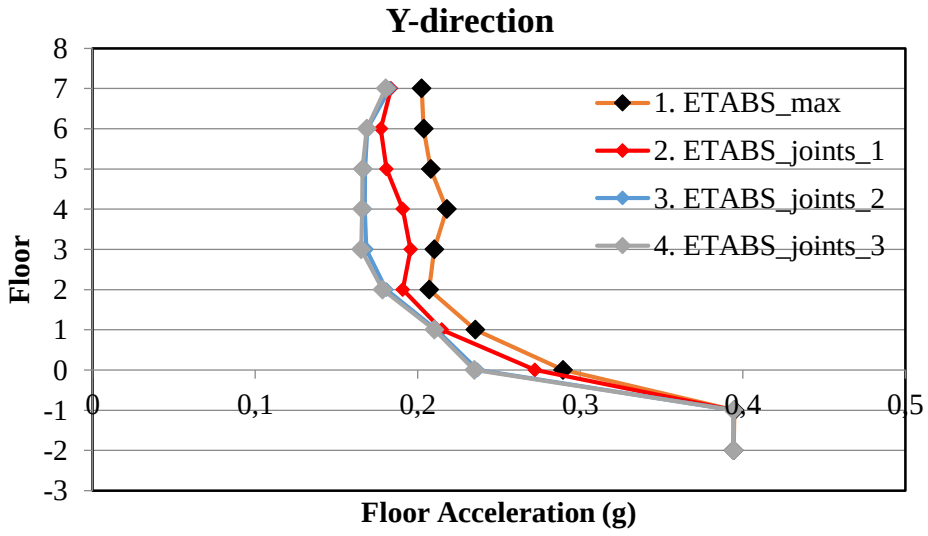
- The rotational movement of the structure also has significant effects on the response